Transferred ^{13}C T_1 Relaxation at Natural Isotopic Abundance: A Practical Method for Determining Site-Specific Changes in Ligand Flexibility upon Binding to a Macromolecule

Steven R. LaPlante,*,†,‡ Norman Aubry,† Robert Déziel,† Feng Ni,‡,§ and Ping Xu*,§

Contribution from Research and Development, Boehringer Ingelheim (Canada) Ltd., 2100 Cunard Street, Laval, Québec, H7S 2G5, Canada, and Biomolecular NMR Laboratory, Biotechnology Research Institute, National Research Council of Canada, 6100 Royalmount Avenue, Montréal, Québec, H4P 2R2, Canada

Received May 22, 2000. Revised Manuscript Received October 2, 2000

Abstract: An NMR strategy is described for measuring changes in ^{13}C spin−lattice relaxation times (T_1) of ligand molecules, at natural isotopic abundance, upon binding to macromolecules of potentially unlimited size. The rapidly reversible binding nature of a substrate-based inhibitor (BILN127SE, $K_i = 5.4\ \mu M$) with the NS3 protease domain of the hepatitis C virus has been well documented and has served as an appropriate system for testing the *transferred* ^{13}C T_1 concept. ^{13}C T_1 relaxation, which is sensitive to motions that occur on the pico- to nanosecond time scale, were first measured for free BILN127SE. Upon addition of the protease at a 25:1 inhibitor-to-protease ratio, differential changes in the ^{13}C T_1 relaxation times of BILN127SE were observed. The equilibrium binding nature of the complex, results in a transfer of T_1 relaxation information of the ligand from the bound to the free state where it is more easily detected. The relative changes in ^{13}C T_1 relaxation provides a qualitative insight into the site-specific changes in ligand immobilization upon binding to the protease. Comparisons of this dynamics information are made with structural data deduced from ^1H NOESY, line-broadening, *J*-coupling, and ROESY experiments. The combination of dynamics and structural information should provide medicinal chemists with further opportunities to design more potent, chemically rigidified inhibitors.

Introduction

The binding of ligands to biological macromolecules involves intricate recognition events that are strongly influenced by ligand structure and dynamics in the free and the macromolecule-bound states. A detailed knowledge of these events would certainly accelerate inhibitor design efforts. NMR and X-ray crystallographic methods have proven to be valuable in determining the structures of ligands when bound to macromolecules; however, the dynamic properties of bound ligands have not been as well characterized. This is partly because few experimental methods can provide this type of information by practical means.

^{13}C T_1 relaxation can provide one of the clearest measurements of atomic-level dynamic behavior of molecules in solution, and it has already served as an important tool for evaluating the internal dynamics of free peptides and inhibitors[1−10] and macromolecules.[11−16] The T_1 relaxation process has already been described theoretically elsewhere.[17−19] Conceptually, the relaxation process occurs via an energy transfer from a ^{13}C nucleus to its surroundings (lattice) and is highly sensitive to the overall tumbling rate of the molecular system and the local motion of the ^{13}C nucleus that occur on the pico- to nanosecond time scales. However, the measurement of T_1 data for macromolecule-bound ligands[20−27] has severe practical limitations. The low sensitivity and natural isotopic-abundance (1.1%) of the

* Corresponding authors. S.R.L.: (telephone) (450) 682-4640; (fax) (450) 682-8434; (e-mail) slaplante@lav.boehringer-ingelheim.com. P.X.: (telephone) (514) 496-5775; (fax) (514) 496-5143; (e-mail) ping.xu@nrc.ca.

† Boehringer Ingelheim (Canada) Ltd.

‡ Also investigator of the Montréal Joint Center for Structural Biology.

§ National Research Council of Canada.

(1) Kessler, H.; Bats, J. W.; Griesinger, C.; Koll, S.; Will, M.; Wagner, K. *J. Am. Chem. Soc.* **1988**, *110*, 1033−1049.

(2) Dellwo, M. J.; Wand, J. *J. Am. Chem. Soc.* **1989**, *111*, 4571−4578.

(3) Palmer, A. G.; Rance, M.; Wright, P. *J. Am. Chem. Soc.* **1991**, *113*, 4371−4380.

(4) Briand, J.; Kopple, K. J. *J. Biol. NMR* **1995**, *6*, 347−360.

(5) Peng, J. W.; Schiffer, C. A.; Xu, P.; Gunsteren, W. F.; Ernst, R. R. *J. Biol. NMR* **1996**, *8*, 453−476.

(6) Zhu, L.; Prendergast, F. G.; Kemple, M. D. *J. Biol. NMR* **1998**, *12*, 133−144.

(7) LaPlante, S. R.; Bonneau, P.; Aubry, N.; Cameron, D. R.; Déziel, R.; Grand-Maître, C.; Plouffe, C.; Tong, L.; Kawai, S. H. *J. Am. Chem. Soc.* **1999**, *121*, 2974−2986.

(8) Friedrichs, M. S.; Stouch, T. R.; Bruccoleri, R. E.; Mueller, L.; Constantine, K. L. *J. Am. Chem. Soc.* **1995**, *117*, 10855−10864.

(9) Ramirez-Alvarado, M.; Daragen, V. A.; Serrano, L.; Mayo, K. H. *Protein Sci*. **1998**, *7*, 720−729.

(10) Daragen, V. A.; Ilyina, E. E.; Fields; Fields, G. B.; Mayo, K. H. *Protein Sci.* **1997**, *6*, 355−363.

(11) Borer, P.; LaPlante, S. R.; Kumar, A.; Zanatta, N.; Martin, A.; Hakkimem, A.; Levy, G. C. *Biochemistry* **1994**, *33*, 2441−2450.

(12) Mispelter, J.; Lefèvre, C.; Adadj, E.; Quiniou, E.; Favaudon, V. J. *J. Biol. NMR* **1995**, *12*, 233−244.

(13) Davis, J. H.; Agard, D. A. *Biochemistry* **1998**, *37*, 7696−7707.

(14) Lee, C.-S.; Kumar, T. K. S.; Lian, L.-Y.; Cheng, J.-W.; Yu, C. *Biochemistry* **1998**, *37*, 155−164.

(15) Kay, L. E.; Muhandiram, D. R.; Wolf, G.; Shoelson, S. E.; Forman-Kay, D. *Nat. Sruct. Biol*. **1998**, *5*, 156−162.

(16) Chatfield, D. C.; Szabo, A.; Brooks, B. R. *J. Am. Chem. Soc.* **1998**, *120*, 5301−5311.

(17) Abragam, A. *The Principles of Nuclear Magnetism*; Clarendon Press: Oxford, England, 1961.

(18) Peng, J. W.; Wagner, G. *J. Magn. Reson.* **1992**, *98*, 308−332.

(19) Peng, J. W.; Wagner, G. *Biochemistry* **1992**, *31*, 8571−8586.

(20) Brewer, C. F.; Sternlicht, H.; Marcus, D. M.; Grollman, A. P. *Biochemistry* **1973**, *12*, 4448−4457.

(21) Candida, F.; Ganadu, M. L.; Guido, C. *Biochem. Pharmacol*. **1983**, *32*, 3241−3243.

(22) Dimicoli, J. L.; Lam-Tanh, H.; Toma, F.; Fermandjiah, S. *Biochemistry* **1984**, *23*, 3173−3180.

10.1021/ja0017817 CCC: $19.00
Published on Web 12/01/2000

magnetically active ^{13}C nucleus requires the use of high sample concentrations and the laborious synthesis of isotopically enriched ligands. The cost of such studies can be further overwhelming since data should be acquired on several different ligand samples that have strategically placed isotopes; isotopically enriched carbons should not be covalently attached to each other for the purpose of reducing the contributions of uninterpretable relaxation pathways. Also, the size of the macromolecule of interest can limit the application of these methods. The line widths of ligands bound to a relatively large macromolecule may be too large to observe the ^{13}C signals directly.

In this work, we propose the use of transferred heteronuclear relaxation measurements as a practical strategy for identifying site-specific changes in flexibility of ligands (at natural isotopic abundance) upon binding to macromolecules. The method is demonstrated using a well-characterized, substrate-based ligand[28−30] upon binding to the NS3 protease domain of the hepatitis C virus.[31]

Materials and Methods

Preparation of NS3 Protease Domain. A clone expressing the HCV serine protease domain of NS3 (amino acid residues 1−180) followed by the amino acid sequence ASKKKK (BK*polyK) was derived from a cDNA fragment of HCV-BK* strain encoding residues 1−189 of HCV NS3 [pET-29b(1−189)]. The expression and purification of the NS3 protease domain (19 800 Da) were performed in a fashion similar to that described elsewhere.[28]

Samples for NMR Studies. NMR samples of free BILN127SE (3 mM for the HSQC T_1 experiment and 4 mM for the HSQC-TOCSY T_1 experiment) were prepared by adding a concentrated solution in DMSO-d_6 to 600 μL of D_2O containing 100 mM sodium phosphate pH 6.5, 300 mM NaCl, and 5 mM DTT-d_{10}. The samples were subjected to a flow of argon gas and then covered or sealed. The samples containing BILN127SE in the presence of the protease (19 800 Da) were prepared in a similar manner except that the protease (19 mg/mL in buffered D_2O) was added such that the final inhibitor-to-protease ratio was 25:1.

The D_2O solution of the protease was carefully prepared by first concentrating the enzyme to the desired volume using Centricon-10 (Millipore) and then centrifuged at 4 °C. The concentrated solution was then transferred into a 0.5-mL QuixSep microdialyzer (Membrane Filtration Products) equipped with a 3500 MWCO dialysis membrane (Spectra/Por, Spectrum Laboratories). Dialysis was performed overnight at 4 °C under a constant blanket of argon gas against 200 mL of D_2O containing 100 mM sodium phosphate pH 6.5, 300 mM NaCl, and 5 mM DTT-d_{10}. The sample was then recovered and the protein concentration determined by an absorbance reading at 280 nm.

NMR Methods. Unless indicated otherwise, all the NMR experiments were recorded at 300 K on a Bruker Avance 800-MHz spectrometer equipped with a 5-mm triple resonance ($^1H/^{13}C/^{15}N$) triple-axis gradient probe. The pulse sequence for the $^1H-^{13}C$ correlation (HSQC) T_1 experiment was similar to that published elsewhere[32] without gradient enhancement. The experiment was specifically set up to measure methyl and methine ^{13}C T_1 times. The HSQC-TOCSY T_1 data were collected using a pulse sequence that applied an HSQC-TOCSY detection module[33] with an isotropic mixing sequence (TOWNY16[34] of 34.69 ms). The pulse program is available upon request and will be published elsewhere.

Spectra were acquired with the ^1H and ^{13}C carrier frequencies set to 4.7 and 39.5 ppm, respectively. They were also acquired with spectral widths of 8741 (^1H) and 2010 Hz (^{13}C) for the HSQC-TOCSY T_1 experiment and with 8741 (^1H) and 3618 Hz (^{13}C) for the HSQC T_1 experiment. There were 2048 complex points (F2) and 36 files (F1) collected. Removal of the HDO solvent resonance was achieved by on-resonance, low-power irradiation during the recycle delay. Carbon decoupling was achieved by the GARP sequence. Phase-sensitive data were acquired in the indirect dimensions by the States-TPPI method. The initial sampling delay in the F1 dimension was set to half the T_1 dwell time[35] to ensure that the aliased resonance signals were either in phase or antiphase as related to the unaliased peaks. Seven T_1 data sets were collected with the following inversion−recovery delays: 2, 90, 190, 300, 480, 700, and 980 ms for the free ligand sample and 2, 45, 105, 185, 285, 415, and 600 ms for the ligand−protease sample. A 180° pulse in the center of the relaxation delay was employed to reduce the contributions of cross-correlation mechanisms between dipole and chemical shift anisotropy relaxation mechanisms.[36,37]

All data were processed using NMRPipe.[38] A 90°-shifted sine square weighting function was used in both dimensions. The time-domain data in T_1 was linear predicted to double the FID's length and then zero filled to 256 points in the carbon dimension. In the proton dimension, the 2048 complex points were zero filled to 4096 points before Fourier transformation. T_1 times were calculated using the following equation: $I(T) = I_0 \exp(-T/T_1)$. I_0 represents the peak intensity at $T = 2$ ms and I is the peak intensity at a delay of time T. T_1 relaxation curves were calculated based on measured cross-peak volumes of the series of HSQC spectra that differed by the relaxation delay values mentioned above. Relaxation times reported here are derived from cross-peaks that were clearly resolved, devoid of overwhelming spectral noise, and for which the calculated T_1 curves described the experimental data with relatively little deviation (<10%).

^{13}C T_1 Relaxation for Ligands Reversibly Bound to Macromolecules in Solution. For rapidly reversible molecular complexes, T_1 values for a ^{13}C resonance averaged between the free and bound states can be calculated using the following equation.[39,40]

$$\frac{1}{T_{1\mathrm{obs}}} = \frac{\alpha_\mathrm{f}}{T_{1\mathrm{f}}} + \frac{\alpha_\mathrm{b}}{T_{1\mathrm{b}} + \tau} \qquad (1)$$

In this equation, T_{1f} is the ^{13}C T_1 relaxation time (in seconds) of the ligand in the absence of a macromolecule. T_{1obs} is the ^{13}C T_1 relaxation time of the ligand in the presence of the macromolecule. The value τ

(23) Fesik, S. W.; Gemmecker, G.; Olejniczak, E. T.; Petros, A. M. *J. Am. Chem. Soc.* **1991**, *113*, 7080−7081.
(24) Lepre, C. A.; Cheng, J. W.; Moore, J. M. *J. Am. Chem. Soc.* **1993**, *115*, 4929−4930.
(25) Fejzo, J.; Lepre, C. A.; Peng, J. W.; Su, M. S.-S.; Thompson, J. A.; Moore, J. M. *Protein Sci.* **1996**, *5*, 1917−1921.
(26) Bortiatynski, J. M.; Hatcher, P. G.; Minard, R. D. *Nucl. Magn. Reson. Spectrosc. Environ. Chem.* **1997**, 26−50.
(27) Zhu, L.; Kurian, E.; Prendergast, F. G.; Kemple, M. D. *Biochemistry* **1999**, *38*, 1554−1561.
(28) LaPlante, S. R.; Cameron, D. R.; Aubry, N.; Lefebvre, S.; Kukolj, G.; Maurice, R.; Thibeault, D.; Lamarre, D.; Llinas-Brunet, M. *J. Biol. Chem.* **1999**, *274*, 18618−18624.
(29) Llinàs-Brunet, M.; Bailey, M.; Fazal, G.; Goulet, S.; Halmos, T.; LaPlante, S.; Maurice, R.; Poirier, M.; Poupart, M.-A.; Thibeault, D.; Wernic, D.; Lamarre, D. *Bioorg. Med. Chem. Lett.* **1998**, *8*, 1713−1718.
(30) Llinàs-Brunet, M.; Bailey, M.; Déziel, R.; Fazal, G.; Gorys, V.; Goulet, S.; Halmos, T.; Maurice, R.; Poirier, M.; Poupart, M.-A.; Rancourt, J.; Thibeault, D.; Wernic, D.; Lamarre, D. *Bioorg. Med. Chem. Lett.* **1998**, *8*, 2719−2724.
(31) See the following for reviews on the molecular characterization of HCV: (a) Bartenschlager, R. *Antiviral Chem. Chemother.* **1997**, *8*, 281−301. (b) Reed, K. E.; Rice, C. M. *Curr. Stud. Hematol. Blood Trans. Basel. Karger.* **1998**, *62*, 1−37.
(32) (a) Farrow, N. A.; Muhandiram, R.; Singer, A. U.; Pascal, S. M.; Kay, C. M.; Gish, G.; Shoelson, S. E.; Pawson, T.; Forman-Kay, J. D.; Kay, L. E. *Biochemistry* **1994**, *33*, 5984−6003. (b) Shaka, A. J.; Parker, P. B.; Freeman, R. *J. Magn. Reson.* **1985**, *64*, 547−552.
(33) Gronenborn, A. M.; Bax, A.; Wingfield, P. T.; Clore, G. M. *FEBS Lett.* **1989**, *243*, 93−98.
(34) Kadkhodaei, M.; Hwang, T. L.; Tang, J.; Shaka, A. J. *J. Magn. Reson., Ser. A* **1993**, *105*, 104−107.
(35) Bax, A.; Ikura, M.; Kay, L. E.; Zhu, G. *J. Magn. Reson.* **1991**, *91*, 174−178.
(36) Boyd, J.; Hommel, U.; Campbell, I. D. *Chem. Phys. Lett.* **1990**, *175*, 477−482.
(37) Wagner, G.; Hyberts, S.; Peng, J. W. In *NMR of Proteins*; Clore, G. M., Gronenborn, A. M., Eds.; CRC Press: Boca Raton, FL, 1993: pp 220−257.
(38) Delaglio, F.; Grzesiek, S.; Vuister, G. W.; Zhu, G.; Pfeifer, J.; Bax, A. *J. Biomol. NMR* **1995**, *6*, 277−293.
(39) Ni, F. *Prog. NMR Spectrom.* **1994**, *26*, 517−606.
(40) Luz, Z; Meiboom, S. *J. Chem. Phys.* **1964**, *40*, 2686−2692.

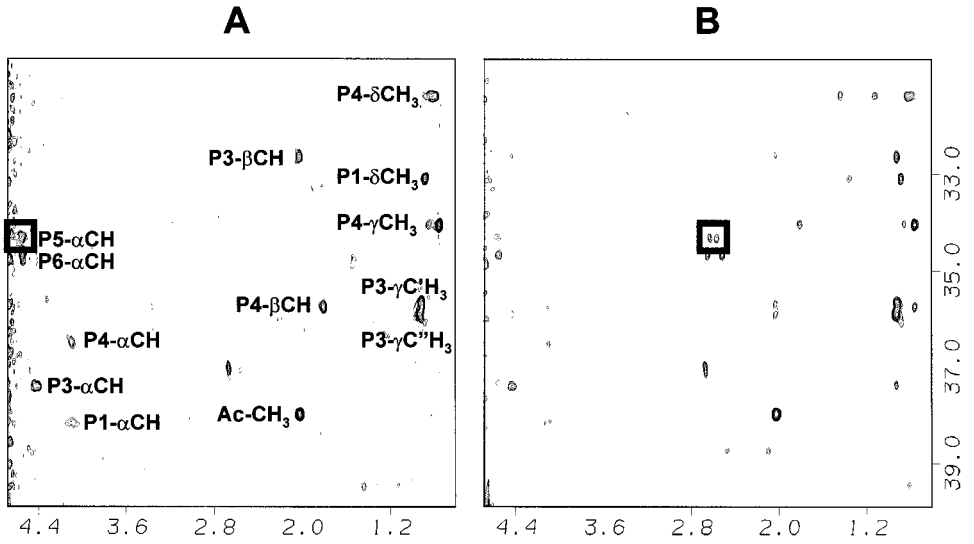

Figure 1. The 2-ms delay ^{13}C T_1 spectra collected at 300 K. (A) HSQC T_1 of 3 mM BILN127SE in the presence of NS3 protease; (B) HSQC-TOCSY T_1 of 4 mM BILN127SE in the presence of NS3 protease (0.16 mM). The horizontal and vertical dimensions are ^1H and ^{13}C, respectively, and are scaled in ppm. The carrier for the ^{13}C dimension was placed at 39.5 ppm with a narrow spectral width to optimize acquisition time and data resolution; spectral widths of 10 and 18 ppm were applied for the HSQC-TOCSY and the HSQC T_1 experiments, respectively. Many of the peaks are folded back and do not truly correspond to the chemical shift values along the axis shown.

Table 1. ^{13}C T_1 Relaxation Data[a] for BILN 127 in the Absence and Presence of HCV Protease BK*PolyK[b]

carbon	^{13}C T_1 free BILN 127 (s)	^{13}C T_1 BILN 127 + protease (s)	change (%)	calcd $T_{1b} + \tau$ (s)
P1−δCH$_3$	0.61	0.40	34.4	0.04
P3−βCH	0.40	0.41	−2.5	1.06
P3−γC″H$_3$	0.22	0.22	0	0.22
P4−βCH	0.45	0.40	11.1	0.10
P4−γCH$_3$	0.30	0.25	16.6	0.05
P4−δCH$_3$	0.40	0.38	5.0	0.17
Ac−CH$_3$	0.55	0.54	1.8	0.37

[a] Data were collected in D_2O solvent. [b] The data were derived from an HSQC T_1 experiment.

represents the lifetime of the complex. Upon addition of the macromolecule, α_f is the fraction of free ligand and α_b is the fraction of bound ligand. Finally, T_{1b} is the ^{13}C T_1 relaxation of the ligand when bound to the macromolecule.

Results and Discussion

^{13}C T_1 of Free BILN127SE. The ^{13}C T_1 relaxation times of free BILN127SE in D_2O solvent were measured by an $^1H-^{13}C$ correlation (HSQC) T_1 experiment which detected protons attached to methyl and methine carbons. T_1 relaxation curves were calculated based on measured cross-peak volumes of a series of HSQC spectra that differed by relaxation delay values. Table 1 lists the relaxation times of carbons for which the resonances were clearly resolved, devoid of overwhelming spectral noise and for which the calculated T_1 curves described the experimental data with relatively little deviation. Clearly, these criteria significantly limited the final data set. For the purpose of trying to augment the data by resolving some of the above encountered problems, a novel HSQC-TOCSY T_1 pulse sequence was designed and found to be useful in practice. For example, the cross-peak volume of the P5−αCH resonance (enclosed in a box in Figure 1A) could not be accurately measured in the HSQC T_1 spectra due to noise introduced at and around the water frequency (4.7 ppm). However, T_1 relaxation times were determined indirectly for P5−αCH in the HSQC-TOCSY T_1 spectra by measuring the two cross-peaks

Table 2. ^{13}C T_1 Relaxation Data[a] for BILN 127 in the Absence and Presence of HCV Protease BK*PolyK[b]

carbon	^{13}C T_1 free BILN 127 (s)	^{13}C T_1 BILN 127 + protease (s)	change (%)	calcd $T_{1b} + \tau$ (s)
P1−αCH	0.39	c		
P1−αCH	0.36	0.31	13.9	0.07
P1−δCH$_3$	0.55	0.36	34.5	0.04
P1−δCH$_3$	0.60	c		
P3−αCH	0.32	0.32	0	0.32
P3−γC′H$_3$	0.19	0.19	0	0.19
P3−γC″H$_3$	0.22	0.20	9.1	0.06
P4−βCH	0.49	0.45	8.2	0.15
P4−γCH$_3$	0.30	0.21	30.0	0.03
P4−γCH$_3$	0.31	0.24	22.6	0.04
P4−δCH$_3$	0.39	c		
P5−αCH	0.48	0.44	8.3	0.14
P5−αCH	0.48	0.40	16.7	0.08

[a] Data were collected in D_2O solvent. [b] The data were derived from an HSQC-TOCSY T_1 experiment. [c] Data not available due to overwhelming spectral noise or the calculated T_1 curves did not describe the experimental data with relatively little deviation.

at the P5−βH and the P5−αC frequencies (enclosed in a box in Figure 1B). The TOCSY segment of the pulse sequence effectively transfers the information to a "cleaner" part of the spectrum where it can be more easily analyzed. Table 2 gives the relaxation times determined from HSQC-TOCSY T_1 data sets. Another benefit of this experiment is that the redundancy of some data values allows a qualitative estimation of the error involved in the T_1 measurements.

The dynamic properties of free BILN127SE were also investigated in DMSO-d_6 solvent by the classical ^{13}C-detected inverse−recovery method. Although this method required high sample concentrations (36 mM BILN127SE), it also offered the advantage of determining the relaxation times of all the protonated carbons within a single set of experiments. Figure 2 shows the ^{13}C NT_1 relaxation data for all the protonated carbons (see the numbers that are not enclosed by parentheses). NT_1 is the product of the number of attached protons and the spin−lattice relaxation time; T_1 values are typically multiplied by the number of attached hydrogens (NT_1) to help in interpreting the

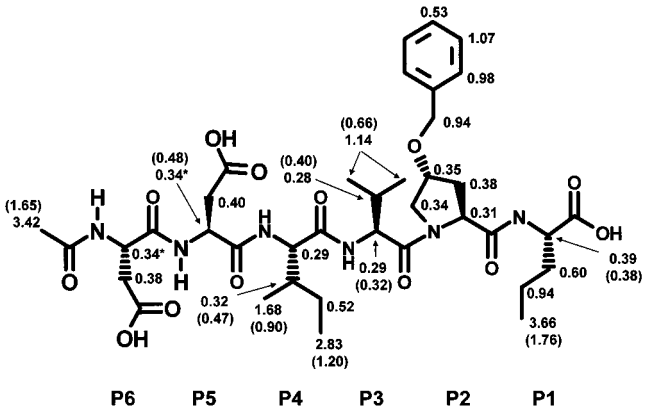

Figure 2. ^{13}C NT_1 relaxation data (collected at 300 K) are shown for free BILN127SE in D_2O solvent (in parentheses) and in DMSO-d_6 solvent[16] (not enclosed by parentheses). NT_1 data (the product of the number of attached protons and the spin−lattice relaxation time) are shown next to the respective carbon atoms. In many cases, the HSQC and HSQC-TOCSY experiments resulted in multiple measurements for the same carbon. In such cases, the average NT_1 value is given. Most of the hydrogens are not displayed for the sake of clarity. An asterisk next to an NT_1 value indicates that resonance overlap was observed for P5 and P4−αCH carbons in the ^{13}C 1-D NMR spectrum. The residues are numbered as shown at the bottom.

relative flexibility between different carbon types. Figure 2 clearly shows that the side-chain protonated carbons have higher NT_1 values than those of the main-chain α-carbons. The data also show higher NT_1 values for $^{13}C-^{1}H$ bond vectors of the side chains that are progressively distant from the relatively rigid backbone. For example, the NT_1 values of P1 increase from the α- to δ-carbons. The nomenclature used to identify residue position is given at the bottom of Figure 2.

Figure 2 also shows a summary of the NT_1 values for free BILN127SE in D_2O solvent (in parentheses). Differences in the relaxation times between the two solvents may be reflective of different local environments (e.g., solvent viscosity, hydrogen bonding, etc).

^{13}C T_1 of BILN127SE in the Presence of NS3 Protease. Our principal goal was to determine whether ^{13}C T_1 relaxation times could be extracted for a ligand at natural ^{13}C isotopic abundance when bound to a protein through rapidly reversible binding. Among other critical factors, testing this would require that the ligand bind to and is released from the macromolecule at a rapid rate; the ^{13}C magnetization of the ligand in the bound state must be transferred to the excess free ligand where it is more easily measured. The fast-exchange binding nature of BILN127SE with NS3 protease in D_2O is illustrated in Figure 3A which shows changes in ^{1}H resonances of BILN127SE upon the incremental addition of the protease. The broadening is derived from site-specific binding based on the resonance-specific nature[39] of the protease-induced line broadening in aqueous buffer as illustrated in Figure 3B. Furthermore, it was only upon addition of the protease to a sample of BILN127SE that transferred NOESY cross-peaks were observed; the transferred NOESY cross-peaks were subsequently lost upon addition of a potent, active-site binding inhibitor to the sample.[28] Also, only a single, bound ^{19}F resonance was identified when a related inhibitor was added to the protease in a 1:1 ratio.[41] Further evidence of resonance averaging between the free and complex forms were found in the $^{1}H-^{13}C$ HSQC and HSQC-TOCSY

(41) LaPlante, S. R.; Aubry, N.; Bonneau, P. R.; Kukolj, G.; Lamarre, D.; Lefebvre, S.; Li, H.; Llinas-Brunet, M.; Plouffe, C.; Cameron, D. R. *Bioorg. Med. Chem. Lett.* **2000**, *10*, 2271−2274.

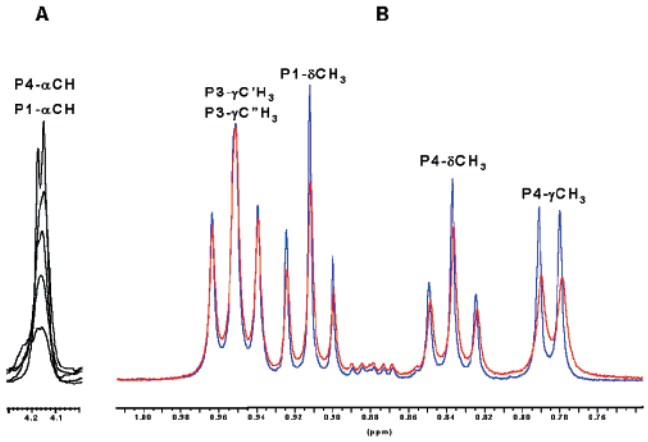

Figure 3. *(A)* NS3 protease-induced increases in the ^{1}H NMR resonance line widths of P4−αH and P1−αH of BILN127SE (3 mM) in D_2O solvent following the incremental addition of the protease at ratios ranging from 53:1 to 13:1 of inhibitor to protease, respectively. (B) Differential line broadening of the ^{1}H NMR methyl region of free 2 mM BILN127SE (blue) and in the presence (red) of NS3 protease (type 1b) at an inhibitor-to-protease ratio of 30:1 in H_2O solvent.[28] The ^{1}H spectra were recorded at 600 MHz and 300 K.

T_1 spectra (data not shown) after addition of NS3 protease where only one cross-peak was identified for each $^{1}H-^{13}C$ bond.

Tables 1 and 2 give the ^{13}C T_1 relaxation times of BILN127SE before and after the addition of the NS3 protease. Differential decreases in the ^{13}C T_1 values were observed which demonstrate that the relaxation-dependent magnetization is successfully being transferred from bound to the excess free ligand. The general decrease in T_1 values was expected given the ratio of free to bound ligand (eq 1) and given the longer tumbling rate expected for the NS3 protease domain (correlation time in the low-nanosecond range[17] for a 19 800 Da protein).

Tables 1 and 2 also provide the percentage change in T_1 times for each carbon upon addition of the protease. The differential changes in T_1 are probably a result of the relatively different degrees of immobilization (vida infra) that each $^{13}C-^{1}H$ bond vector undergoes upon binding the protease. Significant decreases in T_1 values were observed for P1−δCH$_3$, P1−αCH, P4−βCH, P4−γCH$_3$, and P5−αCH, which suggests that these $^{13}C-^{1}H$ bond vectors may undergo significant decreases in flexibility upon binding the protease. On the other hand, no significant changes in T_1 values were observed for P3−αCH, P3−βCH, P3−γC′H$_3$, P3−γC″H$_3$, P4−δCH$_3$, and Ac−CH$_3$, which suggests that these $^{13}C-^{1}H$ bond vectors may not undergo significant immobilization upon binding to the protease.

The apparent protease-bound T_1 values ($T_{1b} + \tau$) of BILN127SE were calculated for the individual $^{13}C-^{1}H$ bond vectors based on eq 1 and on the experimental data given in Tables 1 and 2. Other important parameters included the fractions of free (∼96.1%) and bound BILN127SE (∼3.9%) that were calculated from the ligand and protein concentrations used and based on the expected saturation of the protein by a ligand having a K_i of 5.4 μM.[28] It should be kept in mind, however, that the calculated $T_{1b} + \tau$ values likely have a significant degree of variability. More accurate $T_{1b} + \tau$ values can be determined using experimental data derived from a series of inhibitor/protease ratios. Nonetheless, the wide range of $T_{1b} + \tau$ values listed in Tables 1 and 2 suggests that individual segments of BILN127SE experience various local dynamic tendencies, rather than an assumed view that a bound ligand experiences a single rigid conformation in the bound state. The wide range is also consistent with the lifetime of the complex

(τ) being significantly shorter than T_{1b}, particularly given the fast-exchange binding nature of this complex.[39] If τ were much longer than T_{1b}, it would be expected that no changes in ligand T_1 values would be observed upon addition of the protease due to extensive relaxation of ligand magnetization before release from the complex, or uniform changes would be observed due to the dominance of τ as described in eq 1.

Comparisons of the ^{13}C T_1 Data with Differential Line Broadening and Structural Information. The binding of BILN127SE to the NS3 protease is a complex process that certainly involves both structural and dynamic contributions of the ligand in the free and bound states. The structural features of both states have been extensively investigated using a combination of homonuclear ^{1}H NMR methods,[28] and comparisons with dynamics information can be made from this work.

The correlation of ^{13}C T_1 relaxation data with internal dynamics can qualitatively be made for aliphatic protonated carbons. At natural isotopic abundance, isolated ^{13}C nuclei relax predominantly via a dipole−dipole mechanism to the covalently attached hydrogen(s) with a 1.09-Å H−C distance. Thus, a qualitative interpretation of the ^{13}C T_1 relaxation data reduces to analysis of the dynamic behavior of the ^{13}C−^{1}H bond vectors as a function of time. The direct relationship between segmental motion of ^{13}C−^{1}H bond vectors and the relative ^{13}C T_1 relaxation times has been used to determine the dynamic behavior of organic molecules[42] and peptides and inhibitors.[1,7] It has been approximated that relatively longer ^{13}C T_1 values are indicative of more mobile ^{13}C−^{1}H bond vectors for small molecules that fall within the extreme narrowing condition.[17,27] More elaborate schemes have been devised for correlating relaxation data with the dynamic properties of molecules. There are examples in which the overall and internal dynamics of free[2−6,43] and bound ligands[24,27] were quantitatively determined using the theoretical *model-free approach*[44] that incorporated ^{13}C T_1 and other relaxation data. An overview of these and other data shows a general, inverse relationship between the observed ^{13}C T_1 relaxation values and the calculated order parameter (S^2); longer T_1 times are generally observed for those vectors for which lower S^2 values were calculated. S^2 describes the spatial restriction of the ^{13}C−^{1}H vectors such that $S^2 = 1$ for a rigid part of the molecule and decreases toward zero for parts that are less ordered. Thus, ^{13}C T_1 relaxation data may be used, in a qualitative fashion, to describe the relative flexibility of ^{13}C−^{1}H vectors of a ligand when bound to a slower, isotropically tumbling macromolecule.

In the free state, NMR structural data[28] (^{1}H NOESY, ROESY, *J*-couplings) show that BILN127SE adopts a predominantly extended conformation, and the ^{13}C T_1 (Figure 2) and the NOESY[28] data show that the backbone is relatively rigid whereas the side chains experience a higher degree of flexibility. In the bound state, transferred NOESY data show that BILN127SE assumes an extended conformation.[28] These data were applied as distance restraints to determine the three-dimensional structure[28] shown in Figure 4. Also given in Figure 4 is a summary of the protease-induced, ^{1}H line-broadening information which, taken together, suggests the surface and sites of BILN127SE that come into contact with the protease active site.[28]

Upon binding the protease, BILN127SE undergoes conformational changes as judged by the differences between the ROESY spectrum of the free state and the transferred NOESY spectrum of the bound state.[28] Many cross-peaks either appear or become more intense in the transferred NOESY spectrum. Most of these changes may be a result of the immobilization of BILN127SE upon binding the protease, which is consistent with the decreases in the ^{13}C T_1 values of BILN127SE upon addition of the protease (Tables 1 and 2).

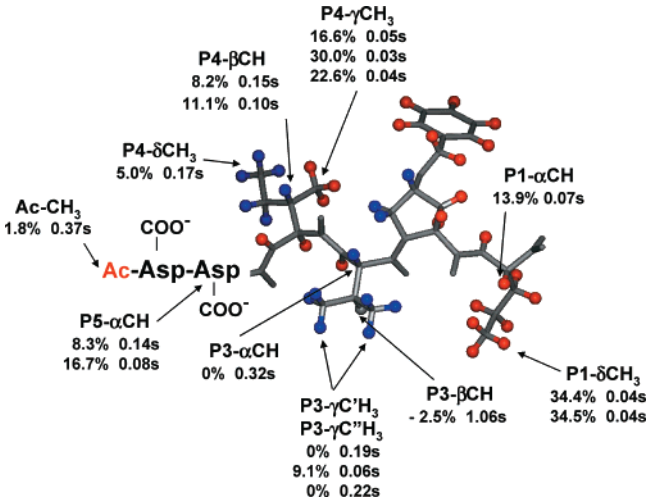

Figure 4. A comparison of dynamic and structural information. Below each assignment is the percentage change in T_1 relaxation of BILN127SE after adding less than a stoichiometric amount of NS3 protease BK*polyK (from Tables 1 and 2). Also shown are the bound T_1 values (seconds) that were calculated using eq 1. Data are given next to the respective carbon atoms on the transferred NOESY-based solution structure of BILN127SE when bound to the NS3 protease. Only the structure of the P1−P4 residues of a representative structure is shown. Also, a qualitative summary of differential line-broadening observations is illustrated on the P1−P4 residues based on comparisons between ^{1}H spectra of BILN127SE in the absence and presence of NS3 protease. Relatively no line broadening was observed for hydrogens colored blue, significant line broadening was observed for hydrogens colored red, and hydrogens were colored gray when resonance overlap hindered a definitive interpretation.

Figure 4 helps illustrate the site-specific correlation between structural and dynamic information. For the most part, those sites that undergo significant changes in ^{13}C T_1 times upon addition of the protease (medium to large percentage values) also exhibit proton resonance line broadening in the presence of the protease (red hydrogens). With few exceptions, these sites are at the proposed interface between BILN127SE and the protease.[28] The site that exhibited the largest change in T_1 upon addition of the protease was P1−δCH$_3$ (34.4%), suggesting that it may undergo the greatest degree of immobilization. The calculated $T_{1b} + \tau$ is also quite low. Although the $T_{1b} + \tau$ value of P1−αCH is similar to that of P1−δCH$_3$, the T_1 of P1−αCH changes less upon adding the protease (13.9%) because the P1−αCH may be less flexible than P1−δCH$_3$ in the free state. Interestingly, a transferred NOESY cross-peak is observed between the hydrogens of these sites, suggesting that they lie in proximity in a common protease pocket. Figure 4 also illustrates that all the hydrogens of P1 experienced significant proton resonance line broadening in the presence of the protease. Medicinal chemistry efforts[29,30] have shown that P1 plays an important role in the interaction of substrate-based ligands with the protease. Analogues that chemically rigidify this residue with an improved affinity for the protease have recently been reported[41] and others will be disclosed at a later date.

In the free state, the side-chain carbons of P3 have the lowest T_1 times for comparable carbons. Upon addition of the protease,

(42) Lyerla, J. R.; Levy, G. C. In *Topic in Carbon-13 NMR Spectroscopy*; Levy, G. C., Ed.; Wiley-Interscience: New York, 1974; pp 79−148.
(43) Beglova, N.; LeSauteur, L.; Ekiel, I.; Saragovis, H. U.; Gehring, K. *J. Biol. Chem*. **1998**, *273*, 23652−23658.
(44) Lipari, G.; Szabo, A. *J. Am. Chem. Soc.* **1982**, *104*, 4546−4559.

these carbons experience little change in T_1. These data and the low calculated $T_{1b} + \tau$ value suggest that P3 is relatively rigid in the free and bound states. Interestingly, the side-chain hydrogens of P3 experience little or no line broadening in the presence of the protease, which may indicate that this side chain has minimal contact with the enzyme. These observations, coupled with the importance of P3 for inhibitory potency,[29] are consistent with the proposal that this bulky side chain plays a major role in rigidifying and predefining the overall extended conformation of the ligand in the free state to resemble that of the bound state.[7,28] This conformational role for the P3 side chain has also been observed for inhibitors of another serine protease,[7] and it may be a general feature for specificity of substrate binding to serine proteases.

The P4 side chain may experience different degrees of immobilization upon binding to the protease. On one hand, the T_1 of P4$-\gamma CH_3$ changes significantly upon adding protease, and the $T_{1b} + \tau$ values are low, whereas only small changes in T_1 are observed for P4$-\delta CH_3$ upon adding the protease, and the $T_{1b} + \tau$ value is relatively high. These observations are consistent with the line-broadening data shown in Figure 4 which suggest that P4$-\gamma CH_3$ contacts the protease whereas P4$-\delta CH_3$ does not to the same extent. This is also consistent with the proposed protease binding face of BILNSE127SE[28] where the P4$-\alpha$CH and P4$-\gamma CH_3$ lie at the interface; the proximity of P4$-\alpha$CH and P4$-\gamma CH_3$ is confirmed by the observation of a transferred NOESY cross-peak between their respective resonances. Consequently, immobilization of the P4$-\gamma CH_3$ group would directly affect the geminal P4$-\beta$CH. This may explain the intermediate $T_{1b} + \tau$ value, the observed changes in T_1, and the lack of hydrogen line broadening for P4$-\beta$CH. As for P4$-\delta CH_3$, it may point away from the binding interface toward solvent.

Upon binding to the protease, the main chain involving P5$-\alpha$CH may experience a decrease in flexibility as suggested by the intermediate $T_{1b} + \tau$ values and changes in T_1 (Tables 1 and 2). This is further supported by the observation of a large P4$-$NH/P5$-\alpha$H cross-peak in the transferred NOESY spectrum.[28] On the other hand, the side chains of P5 and P6 likely experience little change in flexibility upon binding the protease given that no transferred NOESY cross-peaks and no protease-induced ^{1}H line broadening were observed.[28] Unfortunately, little ^{13}C T_1 information could be obtained for the P6, P5, and P2 residues. The N-terminal acetyl group (Ac) experiences limited immobilization upon binding the protease. The $T_{1b} + \tau$ values are high, and there is only a small change in T_1 upon adding the protease. The observed line broadening upon addition of the protease may be due to differences in chemical shifts between the free and bound states rather due to a significant degree of immobilization.

Conclusions

This work introduces a practical method for measuring changes in ^{13}C T_1 relaxation times of a ligand, at natural ^{13}C isotopic abundance, upon binding to a macromolecule. The method provides site-specific dynamic information and, in combination with other structural data, can be valuable for a better understanding of the interactions of ligands with macromolecules. It may also be important for the design of more potent inhibitors in that one could envision an improvement in potency for designed inhibitors that avoid the entropic cost of ligand rigidification upon binding to a target macromolecule.

The relative ease and practicality of the method can greatly simplify the measurement of relaxation data for studying the dynamics of rapidly reversible ligands when bound to a target macromolecule. Transferred ^{13}C T_1 measurements do not require isotopic enrichment and avoid lengthy and costly syntheses. The nature in which the experiment is carried out lends itself to requiring only relatively small amounts of protein and ligand. The method may be applied to macromolecules of potentially unlimited size.

In some respects, the transferred ^{13}C T_1 method can be viewed as a dynamics analogue of the transferred NOESY method.[39] Many of the same physical and experimental requirements apply to both (e.g., detection via excess ligand, rapid and reversible binding, and negligible contributions from nonspecific binding). However, there are important distinctions. The transferred NOESY method has been applied for extracting structural information, whereas the transferred ^{13}C T_1 method will be applied for extracting dynamics information. Due to the multiparameter T_1 minimum effect,[17,43] the observed changes will depend on the bound ^{13}C T_1 values, which are affected by the correlation times of the individual $^{13}C-^1H$ vectors, the correlation time of the macromolecule, and the magnetic field used for data acquisition. Upon addition of the macromolecule, the ligand ^{13}C T_1 values may decrease (as observed here), increase, or change very little. Thus, application of the transferred ^{13}C T_1 method should be preceded by a determination of the range of T_1 values expected for a ligand bound to the macromolecule of interest. Reference 11 shows convenient diagrams that can serve as an initial guide.

Further work is underway which includes the following: (1) HSQC experiments that focus on methylene and aromatic carbons, (2) data accumulation at a range of ratios of ligand to macromolecule, and (3) extension of the method to other heteronuclear relaxation parameters such as heteronuclear NOE and spin$-$spin relaxation.

Abbreviations: HCV, hepatitis C virus; NS3 protease, nonstructural protein 3 of HCV; DMSO, dimethyl sulfoxide; TSP, (trimethylsilyl) propionate-2,2,3,3-d_4; ^{1}H NMR, proton nuclear magnetic resonance; ^{13}C NMR, carbon nuclear magnetic resonance; FID, free induction decay; DTT, dithiothreitol; T_1, spin$-$lattice (longitudinal) relaxation, NT_1, spin$-$lattice relaxation multiplied by the number of covalently attached hydrogens; NOESY, nuclear Overhauser enhancement spectroscopy; HSQC, heteronuclear single-quantum coherence spectroscopy; TOCSY, total correlation spectroscopy; ROESY, rotating frame Overhauser enhancement spectroscopy; TPPI, time proportional phase incrementation; ppm, parts per million.

Acknowledgment. We thank Céline Plouffe, Hong Li, and Dr. Pierre Bonneau for providing the samples of the NS3 protease domain. We are grateful to Drs. Dale Cameron, Nathalie Goudreau, and Stephen Kawai for helpful discussions and critical review of the manuscript. Finally, we thank Drs. Paul Anderson, Michael Cordingley, Michael Bös, Daniel Lamarre, George Kukolj, and Montse Llinas Brunet for encouragement and support. We also thank the reviewers for their help and suggestions.

JA0017817